IL NUOVO CIMENTO Vol. 25 C, N. 2 Marzo-Aprile 2002

An analysis of drought in Italy in the last fifty years(*)

I. Bordi and A. Sutera

Dipartimento di Fisica, Università di Roma "La Sapienza" - Roma, Italy

(ricevuto il 3 Novembre 2000; revisionato il 3 Settembre 2001; approvato il 18 Settembre 2001)

Summary. — In this paper the authors present a study of drought occurrence over Italy. The NCEP/NCAR reanalysis precipitation rates covering the period from 1948 to 2000 were used to assess drought over the area in question. The analysis is based on the Standardized Precipitation Index (SPI), which has been proposed as an indicator of drought occurrence. The index relies on the knowledge of the precipitation field only, therefore, it may be readily computed from the data. A Principal Component Analysis (PCA) of the resulting fields reveals a downward trend for the index over the area considered. It implies that drought conditions have been in the recent past more frequent and extended, within the region, over larger areas. Moreover, the temporal behaviours of the principal component scores show few long-term periodicities.

PACS 92.60.Ry – Climatology.
PACS 92.60.Jq – Water in the atmosphere (humidity, clouds, evaporation, precipitation).

1. – Introduction

Drought is a climatic phenomenon that mostly describes a persistent deficit of precipitation, usually of a long duration, in a particular area. Unlike the aridity, which is a permanent feature of climate, drought may occur also in regions where a large amount of precipitation is the normal condition.

The impact of a drought period has far-reaching consequences affecting many sectors of the production cycle. For this reason, a drought early warning allows optimal planning of water resources, while the knowledge of its time history allows a rationale for measures intended to mitigate the adverse impacts of future occurrences.

An objective evaluation of a drought condition in a particular area requires the design of indices that are able to capture both the water supply deficit and the time duration of this shortage. In general, drought indices are based on precipitation amount and they

(*) The authors of this paper have agreed to not receive the proofs for correction.

may differ in other climatological parameters (such as temperature, pressure, evapotranspiration and soil moisture) that are taken into account.

As already mentioned, drought may occur in regions where large amount of precipitation occurs on average, therefore, in comparing these areas to those with relatively small amount of averaged precipitation, it is important that drought indices are normalised.

Among drought indices (see Bordi *et al.* [1] for an introductory review) the Palmer Drought Severity Index (PDSI) [2] has been widely used for the drought characterisation over an area. Recently, the Standardized Precipitation Index (SPI) [3, 4] has been proposed as an alternative measure of drought occurrence. The latter index is based on the precipitation field alone and, unlike the Palmer index, it is a normalised quantity. The index, at a particular time and in a given location, is defined as a normal variable, a property that greatly helps to interpret results of the analysis that will be presented in the next sections.

In the present paper we will describe the computation of the SPI for a region centred on the Italian territory. The aim of this analysis is to describe the spatial and temporal variability of drought events during the past fifty years. Differently from other fields not similarly conceived, the SPI is a Gaussian field. Thus, the understanding of its covariance field structure exhausts the study of the associated probability density distribution; thereby, our analysis will focus on displaying and interpreting the observed covariances.

The input row data needed for the SPI computation are daily precipitation fields that have been retrieved from the NCEP/NCAR (National Centers for Environmental Prediction/National Center for Atmospheric Research) reanalysis for the period from January 1948 to August 2000. These fields are 1.9×1.9 degrees in longitude and latitude gridded precipitation rates, which have been derived from the primary meteorological fields by means of an assimilating model. Details about the assimilation model and the reanalysis project can be found in Kalnay *et al.* [5]. We did use NCEP/NCAR daily reanalysis both for its time extension and because the data are easily (differently from other centres) accessible through the net. Trenberth and Guillemot [6] have pointed out some of the shortcomings of the NCEP/NCAR precipitation fields, especially in the Tropical regions. However, from their study, midlatitudes features have been compared favourably with other climatologies. Since our study is restricted to the latter regions we may feel enough confidence about the data quality. Moreover, a comparison (here not discussed to keep the paper focused) between the analysis presented and that obtained by using other source of data, such as Dai data set [7] and rain gauge observations, has shown a good agreement. However, the previous data sets, or others similarly conceived, have gaps for many consecutive months. This leaves open the question about the method used in filling these gaps. We stress that, while for other statistics few compromises are foreseeable, in computing the SPI a continuous precipitation record is needed. The same analysis, in fact, with a record having wide gaps may be misleading. Thereby, we think that the NCEP/NCAR reanalysis is optimal for our aims.

The paper is organised as follows. In the next section we will describe the algorithm for computing the SPI and, as an example, we will display the drought condition in Italy for the month of August 2000. In sect. **3** the Principal Component Analysis of the SPI field for the last fifty years will be presented and a trend will be unveiled. In sect. **4** a simple power spectral analysis for few of the most dominant drought behaviours are presented and attempts to connect the found periodicities with the known low-frequency climate phenomena will be offered. Conclusions and an outline of a future work will be contained in the final section.

2. – SPI definition and computation

The method of computing the SPI may be found, for example, in Guttman (l.c.). Nevertheless, for the sake of completeness, we will describe the main steps for computing the index.

The SPI algorithm is based on the assumption that the cumulative precipitation over a period (from few weeks till to few years) is a random variable that is gamma distributed. This assumption may be not fully verified for the data sample here analysed. However, as shown by Guttman (l.c.), it performs among the best probability distribution choices when it is used to compute the SPI. Thereby, if x is the random variable, the gamma distribution is defined by its probability density function as

$$g(x) = \frac{1}{\beta^{\alpha}\,\Gamma(\alpha)}\, x^{\alpha-1}\, e^{-x/\beta} \quad \text{for } x > 0\,, \tag{1}$$

where $\alpha > 0$ is a shape parameter, $\beta > 0$ is a scale parameter and $\Gamma(\alpha)$ is the gamma-function.

The parameters of the gamma probability density function may be estimated from the data sample by means of a maximum-likelihood method for each station, for each time scale of interest and for each month of the year. Thus, we get

$$\tilde{\alpha} = \frac{1}{4\,A}\left(1 + \sqrt{1 + \frac{4\,A}{3}}\right), \quad \tilde{\beta} = \frac{\bar{x}}{\tilde{\alpha}}\,, \tag{2}$$

where

$$A = \ln(\bar{x}) - \frac{\sum \ln(x)}{n}\,, \tag{3}$$

with n the number of observations in which some precipitation has occurred. In addition $\bar{x}$, given a particular month, is the mean of the cumulative precipitation computed for the same month for the different years in the record.

The resulting parameters are then used to find the cumulative probability of precipitation for a given month and time scale at the station considered. The cumulative probability, letting $t = x/\tilde{\beta}$, becomes the incomplete gamma-function:

$$G(x) = \int_0^x g(x)\,\mathrm{d}x = \frac{1}{\Gamma(\tilde{\alpha})}\int_0^x t^{\tilde{\alpha}-1}\, e^{-t}\,\mathrm{d}t\,. \tag{4}$$

Since the gamma-function is undefined for $x = 0$ and the precipitation field may contain zeros, the cumulative probability becomes

$$H(x) = q + (1 - q)\, G(x)\,, \tag{5}$$

where q is the probability of zero precipitation.

TABLE I. – *Classification of the SPI value.*

SPI value	Class
> 2	Extremely wet
1.5 to 1.99	Very wet
1.0 to 1.49	Moderately wet
−0.99 to 0.99	Near normal
−1 to −1.49	Moderately dry
−1.5 to −1.99	Severely dry
< -2	Extremely dry

$H(x)$ is then transformed to a normal variable Z by means of the following approximation [8]:

$$
\begin{aligned}
Z = \mathrm{SPI} &= -\left(t - \frac{c_0 + c_1 t + c_2 t^2}{1 + d_1 t + d_2 t^2 + d_3 t^3}\right) \quad \text{for } 0 < H(x) \leqslant 0.5\,, \\
Z = \mathrm{SPI} &= +\left(t - \frac{c_0 + c_1 t + c_2 t^2}{1 + d_1 t + d_2 t^2 + d_3 t^3}\right) \quad \text{for } 0.5 < H(x) < 1\,,
\end{aligned} \tag{6}
$$

where

$$
\begin{aligned}
t &= \sqrt{\ln\left(\frac{1}{(H(x))^2}\right)} \quad \text{for } 0 < H(x) \leqslant 0.5\,, \\
t &= \sqrt{\ln\left(\frac{1}{(1.0 - H(x))^2}\right)} \quad \text{for } 0.5 < H(x) < 1.0
\end{aligned} \tag{7}
$$

and $c_0,\ c_1,\ c_2,\ d_1,\ d_2,\ d_3$ are the following constants:

$$
\begin{aligned}
c_0 &= 2.515517\,, \qquad d_1 = 1.432788\,, \\
c_1 &= 0.802853\,, \qquad d_2 = 0.189269\,, \\
c_2 &= 0.010328\,, \qquad d_3 = 0.001308\,.
\end{aligned} \tag{8}
$$

Hence, the SPI represents a *Z*-score or the number of standard deviations (above or below) that an event deviates from the mean. At a given time, the SPI may be computed on different time scales, say one month or longer, just by computing the cumulative probability at a given location for the time scale considered. Usually, 3, 6, 12 and 24-months time scales are selected to give information about the drought condition over an area and its impacts on different segments of the hydrological cycle. These time scales, in fact, reflect the impact of drought on the availability of the different water resources, such as soil moisture, ground water and reservoir storage. The classification of dry and wet events intensities resulting from the SPI computation is shown in table I.

As an example, we show in fig. 1 the SPI fields for the Italian region (*i.e.* 7.6°E-19°E, 35.1°N-48.4°N) for the month of August 2000 and for 3, 6, 12 and 24-months time scales, respectively.

A visual inspection of the figures show that on a 3-month time scale all the Italian regions are characterised by near normal conditions, while Apulia and Calabria are in moderately dry conditions. This suggests that, on shorter time scale, the occurrence of wet events is sufficient to balance the precipitation deficit in most parts of Italy. On a

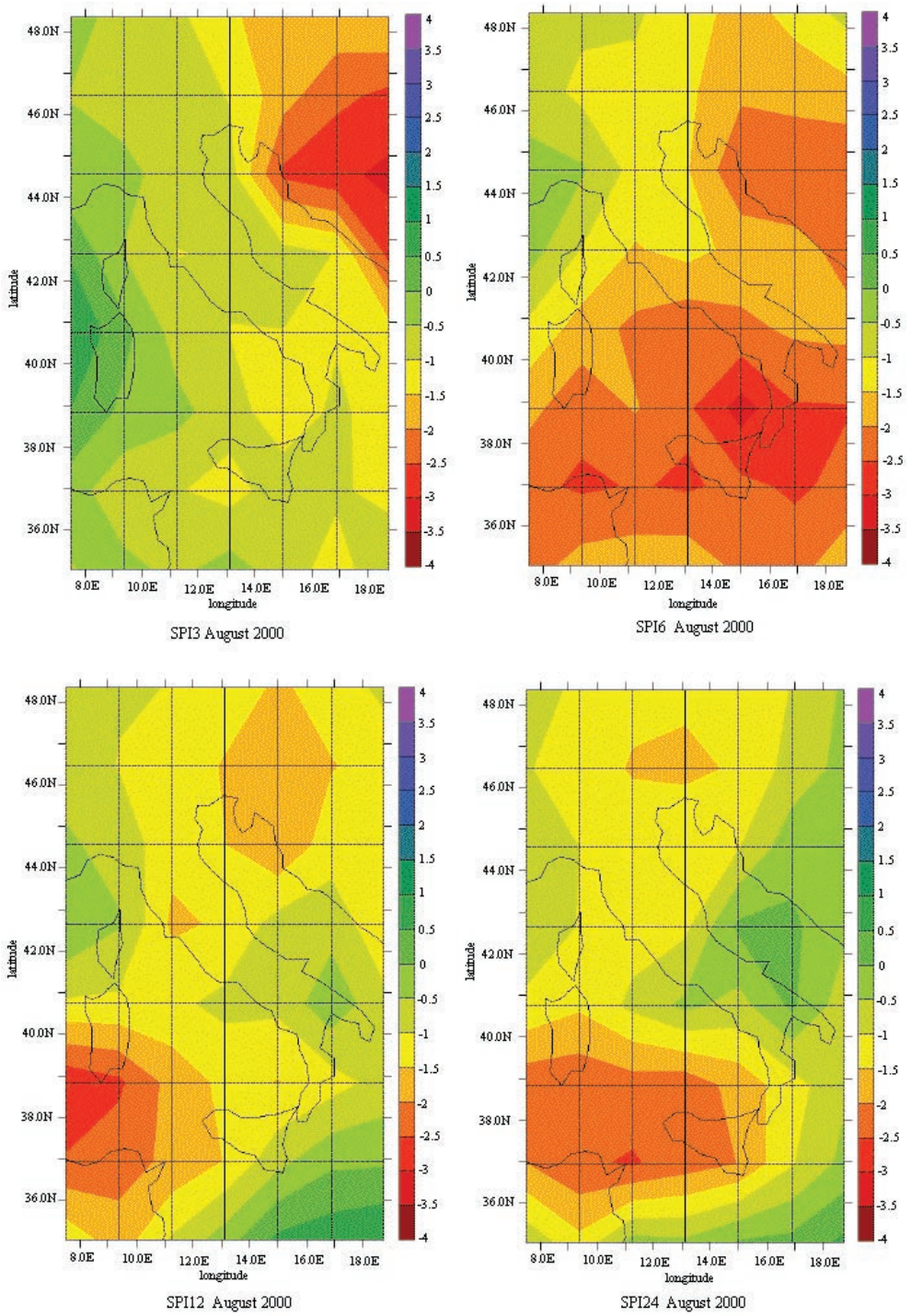

Fig. 1. – SPI for Italy on 3-month (upper left), 6-month (upper right), 12-month (lower left) and 24-month (lower right) time scales. Computations refer to August 2000.

6-month time scale the northern side of Italy features a moderately dry or near normal condition, while southern regions are affected by severe or extreme droughts. On longer time scales (12 and 24 months) the unbalance remains even if it is less marked. The central regions, in fact, are in normal or moderately wet conditions, while Sardinia and Sicily are affected by a severe drought. This means that Sicily and Sardinia are probably affected by hydrological drought, with consequent loss of water resources.

It must be noted that, by definition, the time scale selected characterises the type of drought monitored (*i.e.* meteorological, agricultural or hydrological drought). Consequently, we may have that a drought occurring on a particular time scale may not happen on the other time scales. In fact, the cumulated precipitation on a particular time scale is weakly dependent on those associated to other time scales.

3. – Some descriptive statistics over the region

In this section we will describe the behaviours of few basic drought-related statistics as deduced from the SPI computation on 3- and 24-month time scales for the period from January 1950 to August 2000.

A gross measure of the area extension of drought can be captured by the percentage of grid points that are in dry condition, say A_{d}, for each month of the record. Let the SPI value less than a given threshold be a measure of drought occurrence, then the area covered by drought is readily computed. The time behaviour of A_{d} is shown in figs. 2a, b for the SPI on a 3- and 24-month time scales, respectively and for the case in which the threshold value of the SPI is set to be -1.

Even at a first glance, figures show that the area covered by drought has increased dramatically (roughly from 10% up to 40% of the total area) during the last 25-30 years, and that the transition occurs rather sharply. It is possible to compute a linear trend for A_{d}:

$$A_{\mathrm{d}} = a\,t + b\,. \tag{9}$$

For our case the coefficients a and b take the values

$$a = (0.599 \pm 0.043)\ \% \cdot \mathrm{y}^{-1}\,, \quad b = (-1168.219 \pm 84.732)\ \% \tag{10}$$

for the 3-month time scale and

$$a = (1.156 \pm 0.037)\ \% \cdot \mathrm{y}^{-1}\,, \quad b = (-2265.865 \pm 73.974)\ \% \tag{11}$$

for a 24-month time scale. The ranges correspond to the 95% confidence limits. We remark that, if the trend in (9) would persist, in less than 100 years from now the whole region will be in a dry condition.

Thus, it appears that drought has a systematic time structure. The study of the temporal and spatial structure of this variability will be the topic covered by the next section. In the following, we will limit computations to the SPI on a 24-month time scale, namely the time scale that mostly describes long-term modification of drought variability.

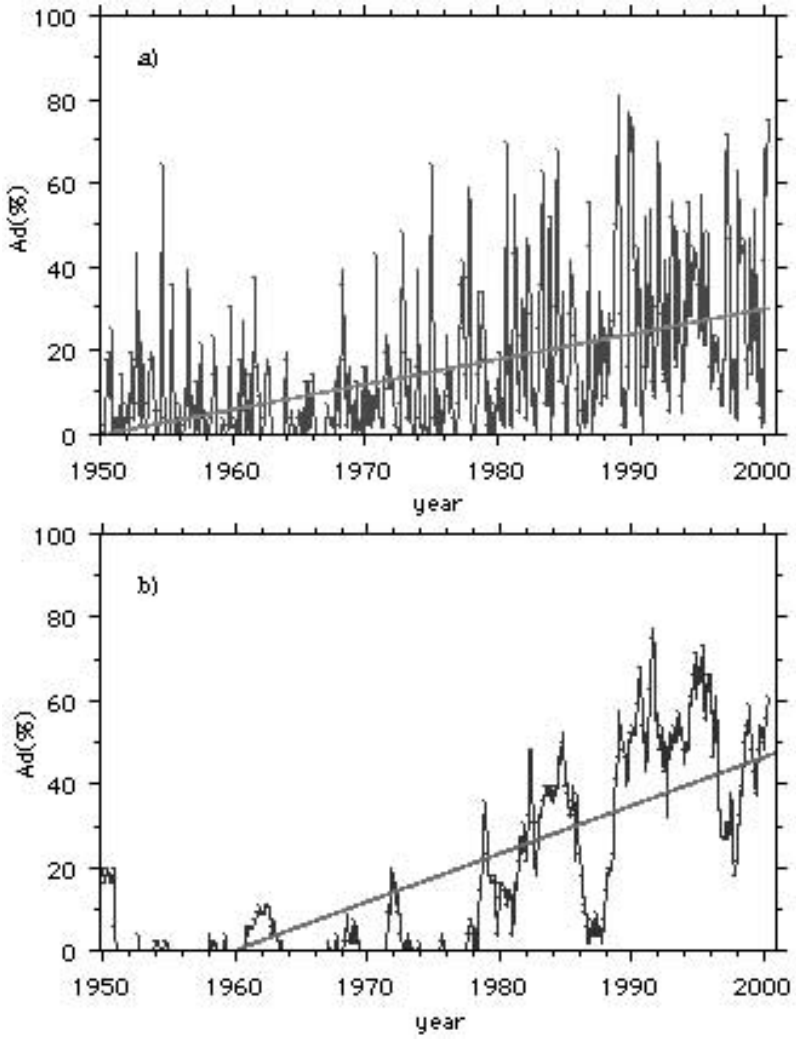

Fig. 2. – a) Percentage of grid points (A_d) where the SPI on a 3-month time scale has values less than -1 as a function of time in years from January 1950 to August 2000. The area analysed is the Italian territory as shown in fig. 1. Straight line denotes the linear regression of A_d. b) As in a) but for the SPI on a 24-month time scale.

4. – Drought patterns and their history in Italy

In spite of the limited number of points where the SPI is sampled, we are dealing with a two-dimensional random field. Dealing with the statistics of a two-dimensional random field of unknown probability may be an insurmountable task. Fortunately, by its own definition, such a field is normal distributed. Thus, its covariance structure completely determines the associated probability distribution. The sample covariance, however, is in our case 56 by 56 matrix, which spans a 56 dimensional space. For the purpose of displaying the main patterns of covariance, some dimensional reduction method is

necessary.

A method that has received acceptance in the meteorological literature (thought, occasionally misused) is the Principal Component Analysis (PCA) [9] of the sample covariance matrix ([10], see also [11] for a study of the covariability of the global geopotential field and [12] for extension to multiple fields analysis). The PCA, sometimes referred to as Empirical Orthogonal Function (EOF) analysis, provides a convenient method for studying the spatial and temporal variability of long-time series of data over large areas.

The method amounts to project the sample data onto the orthonormal eigenfunctions of the covariance matrix. Since this matrix is real symmetric and semi-positive definite, its eigenvalues are positive. This means that each eigenvalue, when it is divided by the trace of the covariance matrix, tells about the explained fraction of the total variance.

Thus, if λ and θ are longitude and latitude, respectively, we have

$$\mathrm{SPI}(\theta,\, \lambda,\, t) = \sum_{n=1}^{N} c_n(t)\, e_n(\theta,\, \lambda)\,, \tag{12}$$

where e_n is the eigenvector of the covariance matrix, $c_n(t)$ are the projection coefficients (or PC scores) and N is the number of spatial observations. Usually, it is useful to display the PCs loading patterns, which are obtained multiplying the eigenvectors by the square root of the associated eigenvalues of the covariance matrix. Under this decomposition, the loading patterns represent the correlations between the PC scores and the observations.

The coefficients of the expansion may be considered as functions of time and they can be obtained by projecting the fields onto the eigenfunctions. These coefficients will be orthogonal in time. To reduce the degrees of freedom we may select few eigenvectors. However, there is no general rule to decide how many eigenvectors should be retained, though few methods have been proposed [13] (Rencher l.c.). For our case, we decided to keep 9 eigenvectors since they capture about 94% of the total variance.

The PCA may be interpreted as the search of the axis along which most of the variance lies. Frequently, it may of some interest to rotate these eigenvectors in a way that a greater portion of variance is retained by the corresponding field, allowing then to select objectively regions of similar drought co-variability. This process requires to multiply the subspace of the selected principal component by a rotation matrix that may lead to an orthogonal or oblique rotation depending whether the rotation matrix is orthogonal or not.

In the present paper only an orthogonal rotation is considered according to the VARIMAX criterion (the algorithm used is FROTA [14]). Of course, each rotated pattern will not explain the same variance of the unrotated principal components although the total variance explained remains unchanged.

On this ground, we have performed PCA of the SPI on a 24-month time scale. The results can be summarised as follows:

– The scree plot is shown in fig. 3;

– Eigenvalues and the variance explained by each of them are listed in table II;

– The loading patterns for the nine unrotated PCs and the associated projection coefficients are shown in figs. 4 and 5, respectively.

The first two points further justify our limitation to nine principal components for the analysis. As is shown in fig. 3 and table II, the eigenvalues decrease quickly toward

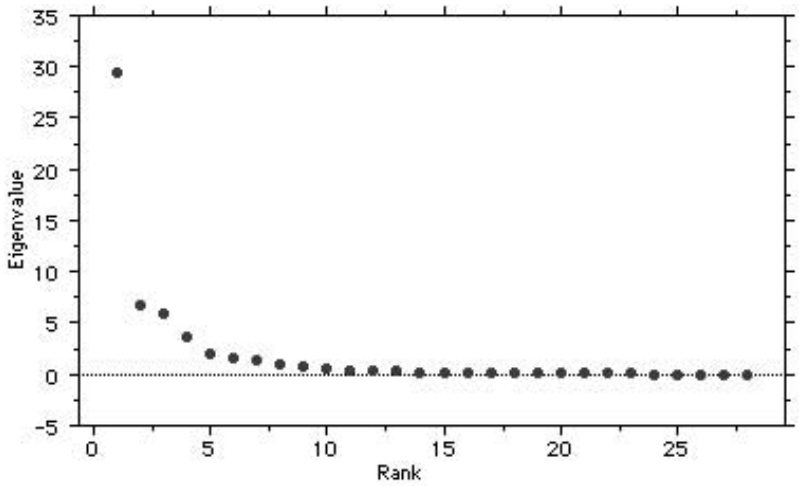

Fig. 3. – Eigenvalues of the covariance matrix for the SPI on a 24-month time scale as a function of the rank.

values close to zero and the nine eigenvectrors selected altogether explain $\approx 94\%$ of the total variance.

Figures 4 and 5 allow few comments. The maps, especially pattern 1, 2, 3 and 4, show higher loadings in certain regions with respect to other areas (values grater than 0.6 and denoted by red contours) meaning high correlations between the corresponding PC scores and the observations in those regions. It must be noted that the first mode, which accounts for 52.7% of the total variance, has a maximum in Calabria, Apulia, Sardinia, eastern Alps and no sign change throughout the domain.

The time behaviour of the factor score associated with the first principal component shows that this pattern has a clear trend towards negative values. Since the pattern is positive everywhere on the region, it implies that the area under analysis from the seventies onward has been more affected by a drought condition. In particular, the southern regions, including Sardinia and Calabria, and the central Alps are the centres

TABLE II. – *First nine eigenvalues (second column) and the corresponding variance contributions (third column) of the PCs scores of the monthly SPI on a 24-month time scale. The cumulative variance is* $\simeq 94\%$.

	Eigenvalue	% variance
1	29.51	52.70
2	6.82	12.18
3	6.01	10.73
4	3.74	6.67
5	2.05	3.66
6	1.53	2.73
7	1.34	2.38
8	1.06	1.90
9	0.78	1.39

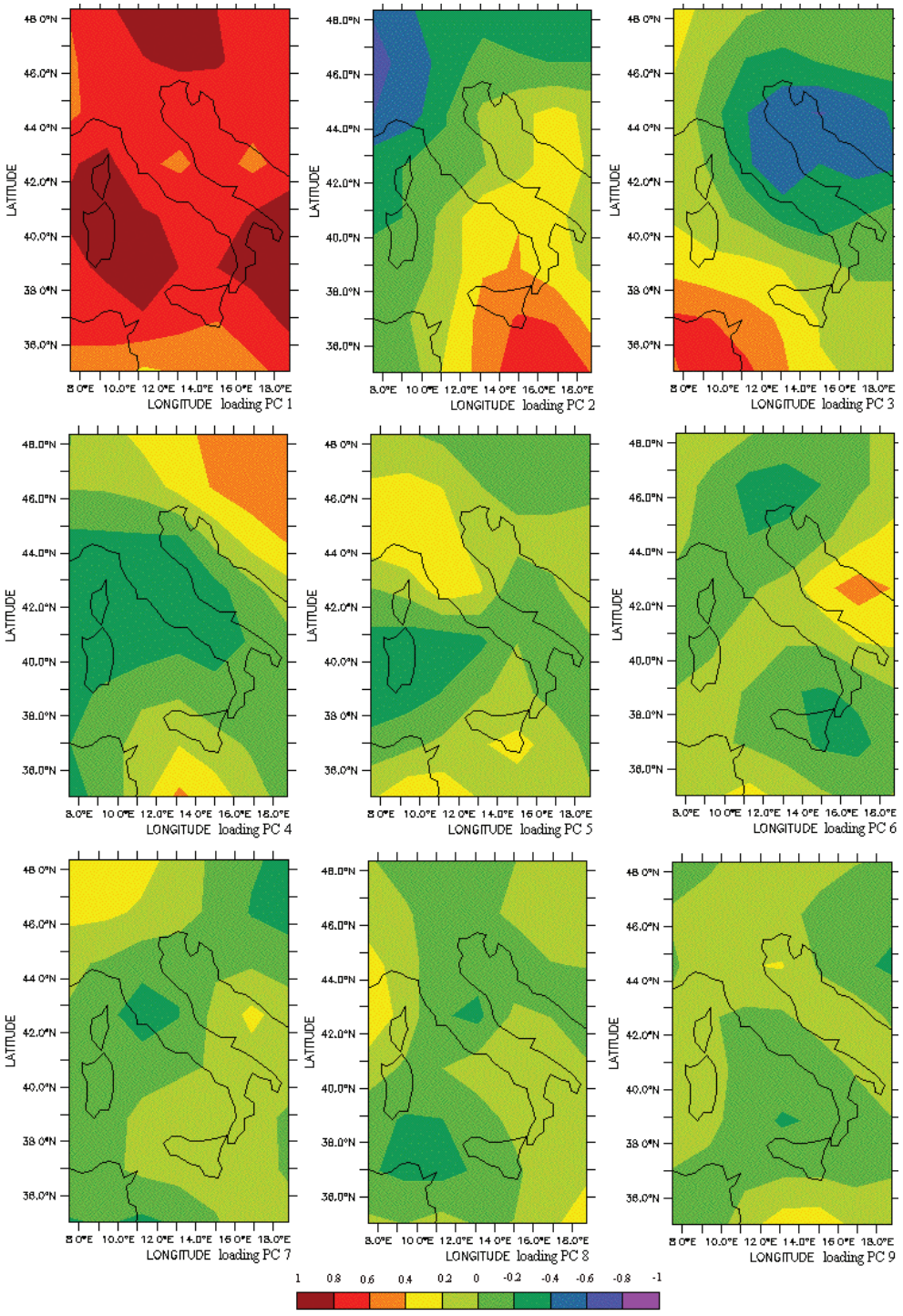

Fig. 4. – Loading patterns of the first nine principal components (PCs) of the SPI field on a 24-month time scale for Italy. Contour interval is 0.2.

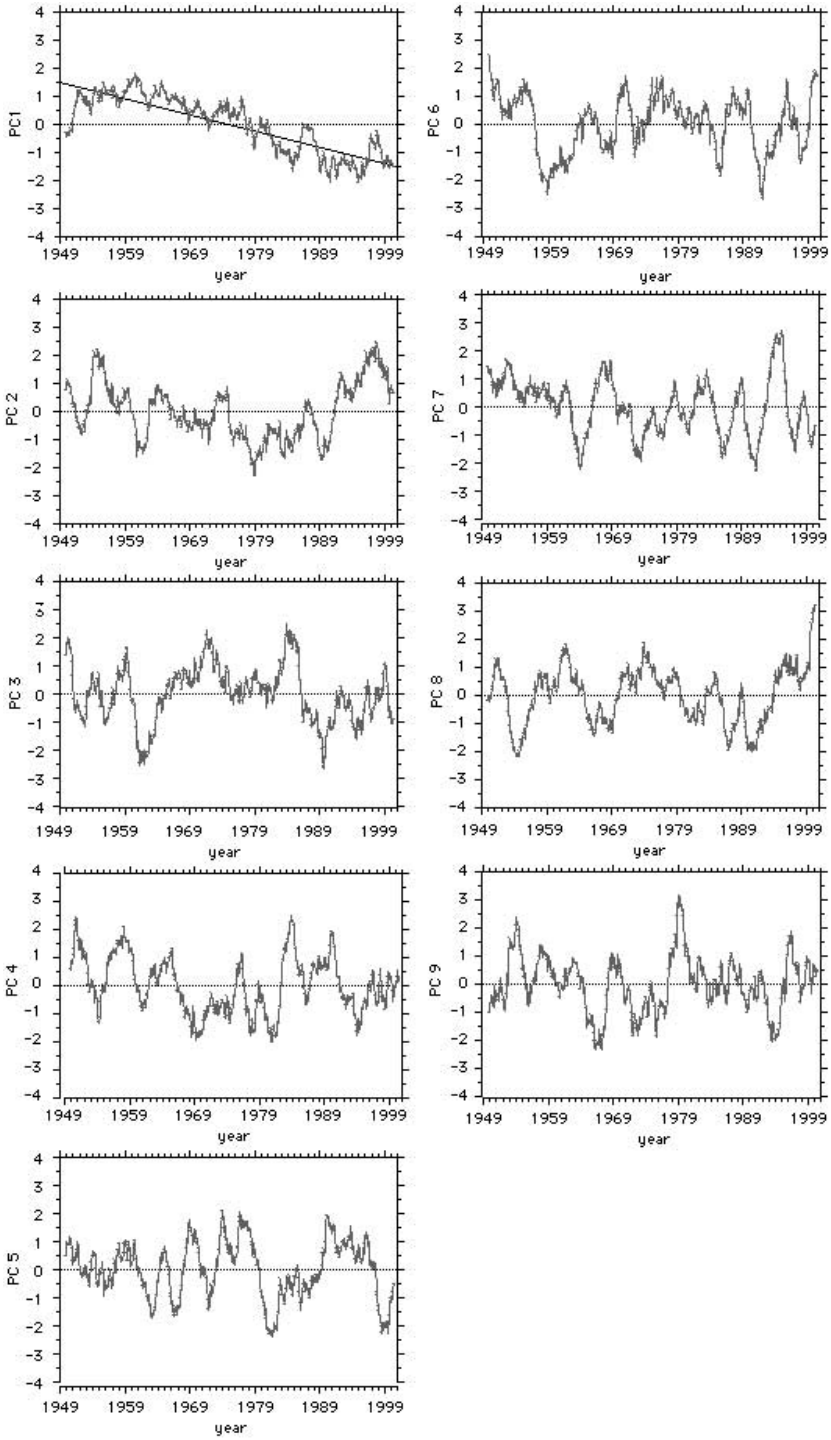

Fig. 5. – Time series of the first nine principal component scores (PCs) of the SPI on a 24-month time scale. Scores are standardised.

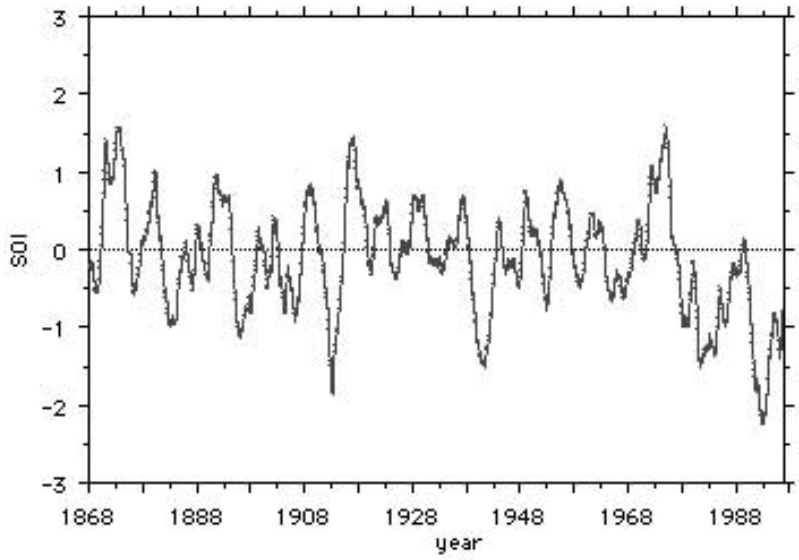

Fig. 6. – Monthly SOI signal from January 1868 to December 1997 as a function of time. A running mean over 48 months has been applied.

that have been hardly affected by this downward trend. It may be shown that the trend unveiled might be a part of a world-wide behaviour that has occurred for the length of the present data record [15]. Details about this argument will be discussed in a follow up paper, here we propose only a preliminary investigation.

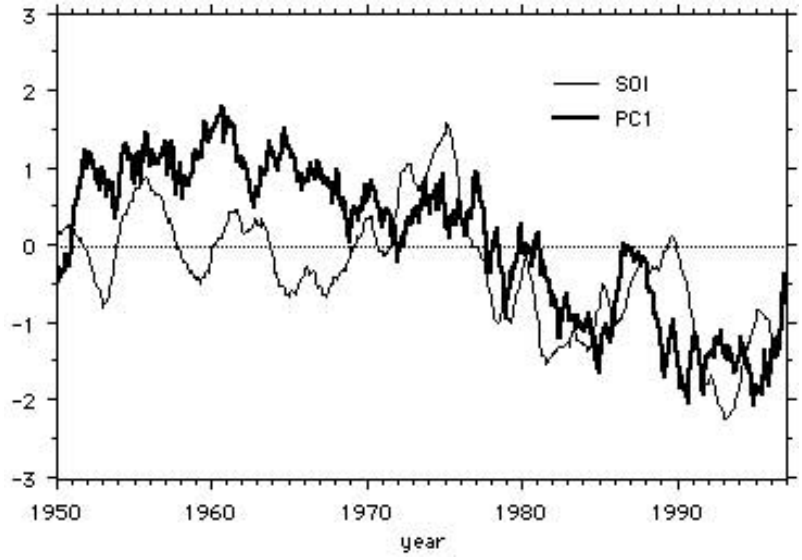

Fig. 7. – SOI signal (thin line) and the first PC score (thick line) as a function of time from January 1950 to December 1997. A running mean over 48 months has been applied to the SOI.

TABLE III. – *First nine eigenvalues (second column) and the corresponding variance contributions (third column) of the unrotated PCs scores of the monthly SPI on a 24-month time scale. Temporal trend on each grid point of the domain has been removed from the SPI values. The cumulative variance is* $\simeq 91\%$.

	Eigenvalue	% variance
1	15.42	27.53
2	11.38	20.33
3	8.67	15.48
4	5.38	9.62
5	3.02	5.39
6	2.44	4.36
7	1.86	3.32
8	1.70	3.03
9	1.18	2.11

Since the leading factor score reveals a multi-year variability, this means that a possible linkage between PC1 and ENSO (El Niño-Southern Oscillation) [7] event could be detectable. We show in fig. 6 the SOI (Southern Oscillation Index [16]) signal from 1868 to 1997. A running mean over 48 months is applied to the SOI signal. As a qualitative analysis, we show in fig. 7 the PC1 (thick line) and the SOI index (thin line) from 1950 to 1997. The resulting correlation coefficient in this case is 0.62 and it is significant at 95% of confidence. The result suggests that there is a linkage of the Tropical Pacific ENSO variability to the temporal behaviour of drought as detected by the SPI computation. However, the consequent influence of ENSO events on the precipitation fields in the Mediterranean area deserves further investigations (see, as an example, [17] for an investigation on the influence of ENSO on drought occurrence in Sicily) on some plausible physical mechanism.

Other general comments might be made about the other patterns. However, since we are attempting a description of the spatial variability of drought filtering out possible climate drifts, some time filtering is required. By inspection of the time series at each location (not shown) it appears that the trend shows considerably variability in the area under analysis.

Therefore, we remove the estimated linear trend at each location (*i.e.* grid point) and analyse the structure of the resulting data covariance matrix. The nine loading patterns and the related time behaviour of the factor scores are presented in figs. 8 and 9, respectively. In table III the percentages of the total variance explained by the nine patterns are summarised. Notice that the first leading mode, which accounts for 27.53% of the variance, is now changed having high values over all the Italian regions with exception of Sicily and western Alps. The temporal behaviour of the leading PC score shows a multi-year fluctuation and indicates the years 1950, 1985 and 1990 as the drier periods of the record in those regions where the first PC spatial mode assumes values at least grater than 0.6.

The second PC mode, which accounts for 20.33% of the variance, remains the pattern where most of the spatial variance is confined in Sicily. The corresponding PC score shows that drier events have occurred in 1961-62, 1979 and 1989, while the last years have not been affected by long-term drought conditions. Similar considerations can be made for the other loading factors and the corresponding factor scores, to describe

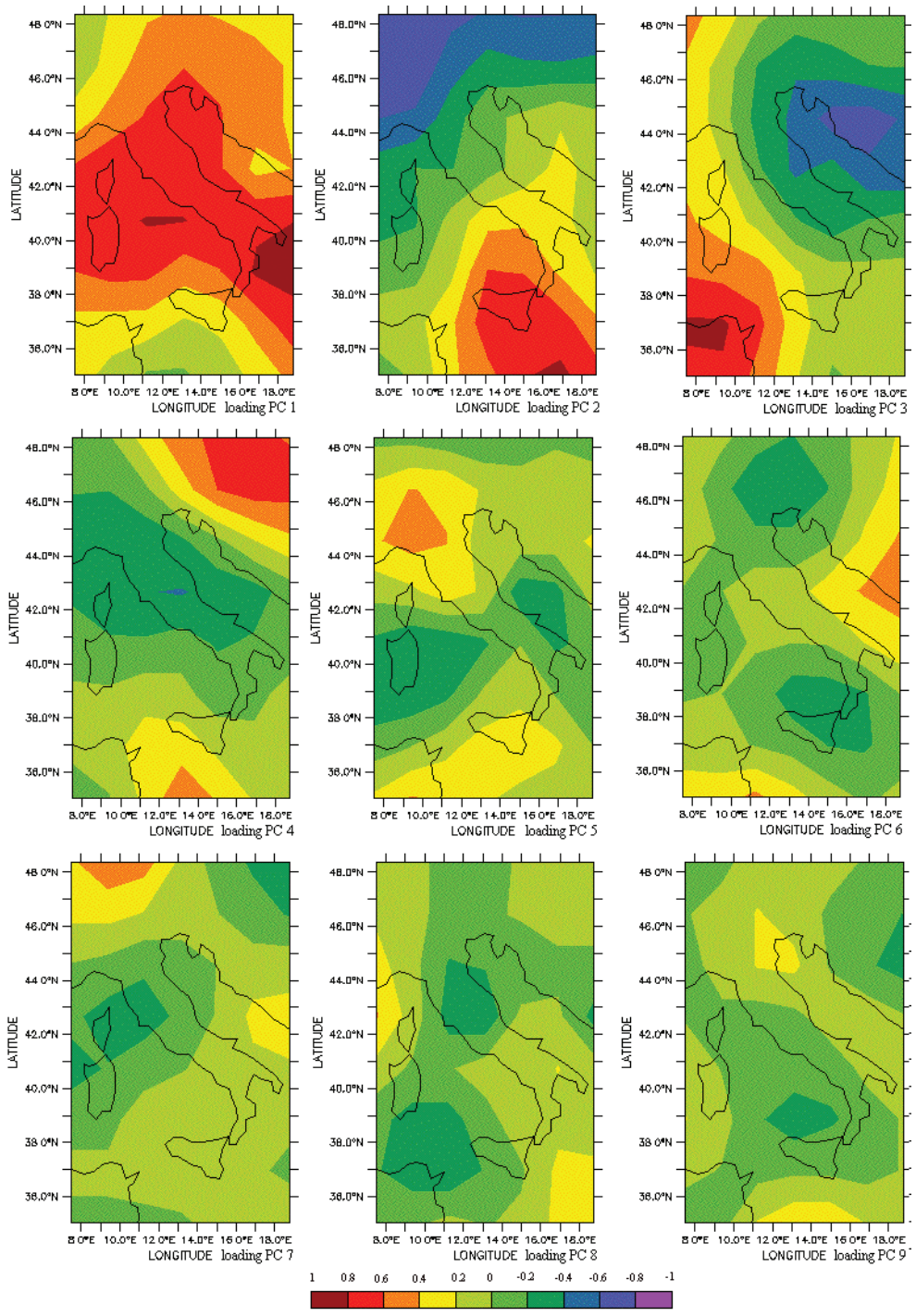

Fig. 8. – Loading patterns of the first nine principal components (PCs) of the SPI field on a 24-month time scale for Italy. The temporal trend at each grid point has been removed. Contour interval is 0.2.

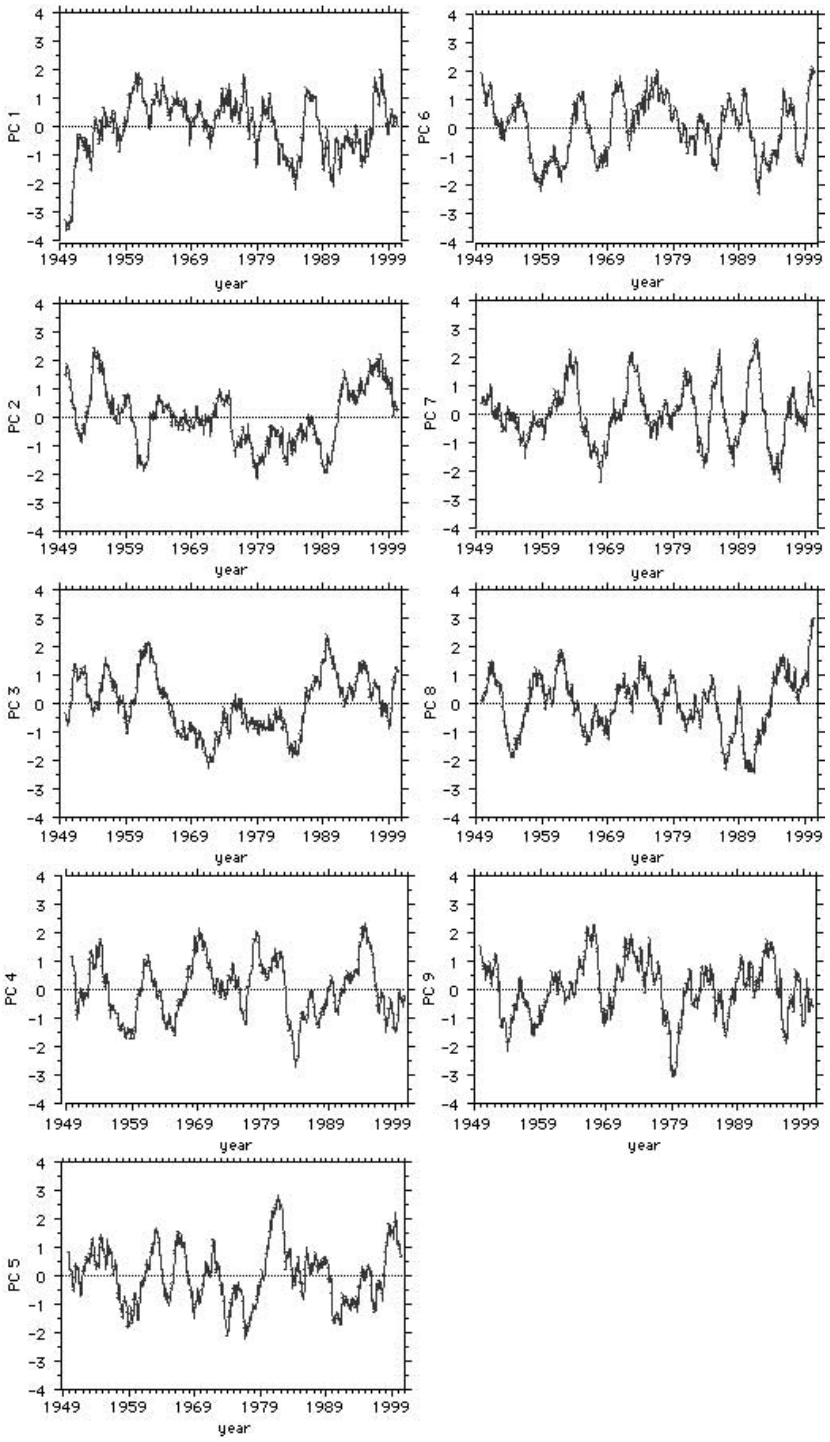

Fig. 9. – Time series of the first nine principal component scores (PCs) of the SPI on a 24-month time scale. The temporal trend at each grid point has been removed. Scores are standardised.

TABLE IV. – *The nine variance contributions (second column) of the VARIMAX rotated PCs scores of the monthly SPI on a 24-month time scale. Temporal trend on each grid point of the domain has been removed from the SPI values. The cumulative variance is* $\simeq 91\%$.

	% variance
1	11.74
2	14.77
3	14.73
4	13.73
5	10.51
6	7.23
7	11.38
8	3.38
9	3.56

drought variability along the years on the other regions of Italy.

Figures 10, 11 and table IV show the loading patterns for the nine orthogonally rotated PCs (RPCs), the time behaviours of the corresponding scores and the percentage of variance explained by each of them. Notice that the rotated PCs become more spatially localised and the variance at each grid point is projected onto fewer modes. The loading spatial mode (11.74% of the total variance) has a maximum on the Adriatic sea basin and the Balkan regions, the second mode (14.77% of the variance) is localised on Sicily, the third (14.73% of the variance) on Sardinia and so on. As in the previous cases, the corresponding RPCs scores show the time behaviours of drought occurrences on these regions. Since the orthogonality of the RPCs scores is conserved under rotation, the time structures of drought events on the nine areas selected by the loading factors are uncorrelated and describe the natural variability of drought when the temporal trend has been removed. For example, Sicily and Sardinia (second and third RPC scores) show a different time behaviour, especially in the last decade.

5. – Spectral analysis of the PC scores

The above results show that, despite the limited temporal coverage of the precipitation data set, a multi-year and decadal variability in the time structures of the 24-month SPI fields is present in the record. Some studies have revealed possible links between solar and/or lunar variability and the regional extent of drought (see, for example, [18-20]). Moreover, recent works have pointed out possible correlations between low-frequency sea surface temperature (SST) fluctuations in the Tropical Atlantic and precipitation fields, at least in the neighbour regions (see, for example, [21]).

The goal of this section is to investigate these arguments. Therefore, we have carried out a preliminary examination of the spectral characteristics of the unrotated PCs scores of the SPI fields on a 24-month time scale where the temporal trend at each grid point has been removed. It must be noted that an analysis on a single grid point would lead to survey 56 spectra. However, we can gain insight by just looking to the nine PC scores spectra, knowing that the geographical regions of maximum co-variability are those selected by the associated loading patterns.

For each of the nine principal component series we have computed the normalised spectral density for the period January 1950 to August 2000 by using the Tukey-Hamming

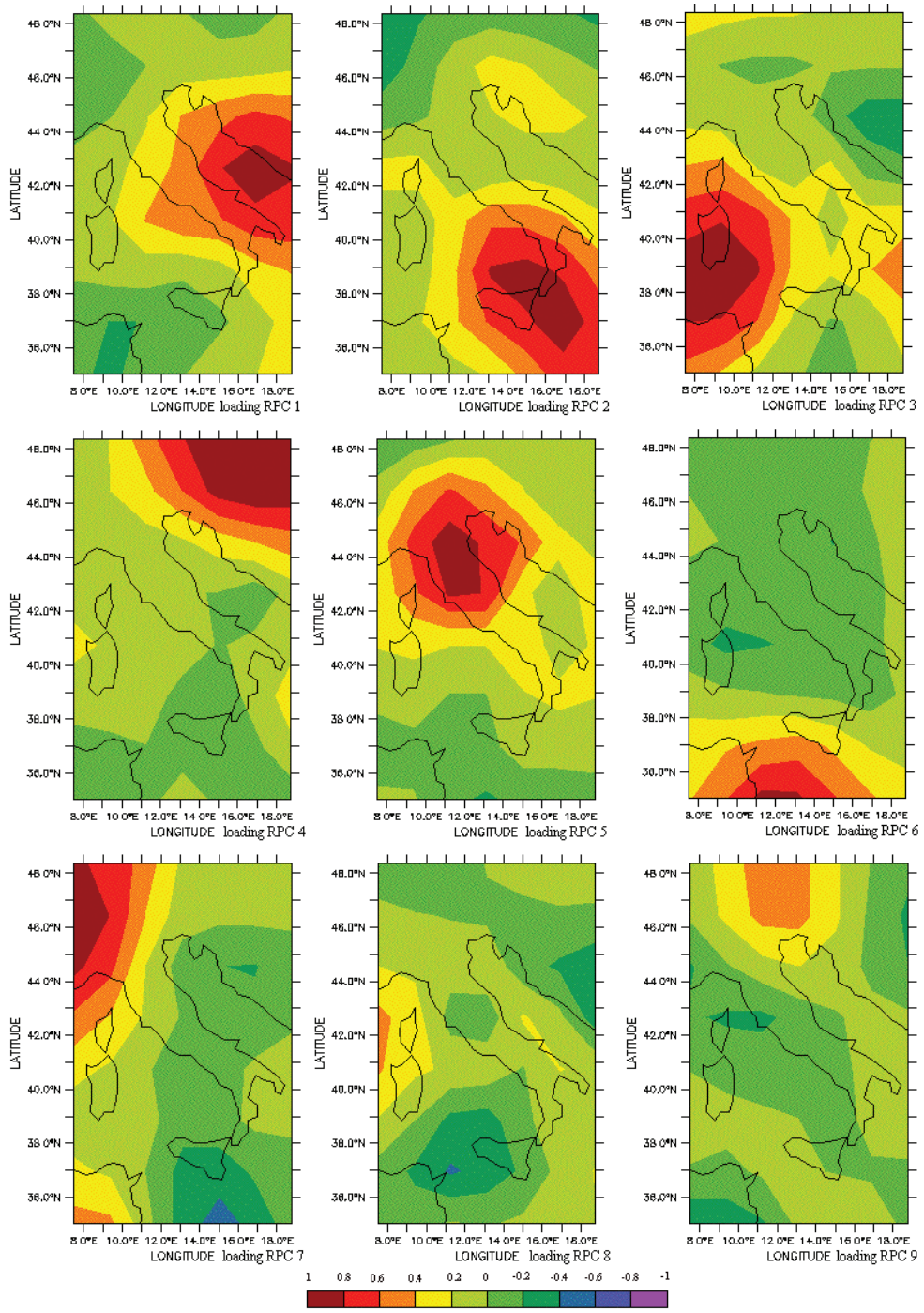

Fig. 10. – Loading patterns of the nine VARIMAX rotated principal components (RPCs) of the SPI on a 24-month time scale for Italy. The temporal trend at each grid point has been removed. Contour interval is 0.2.

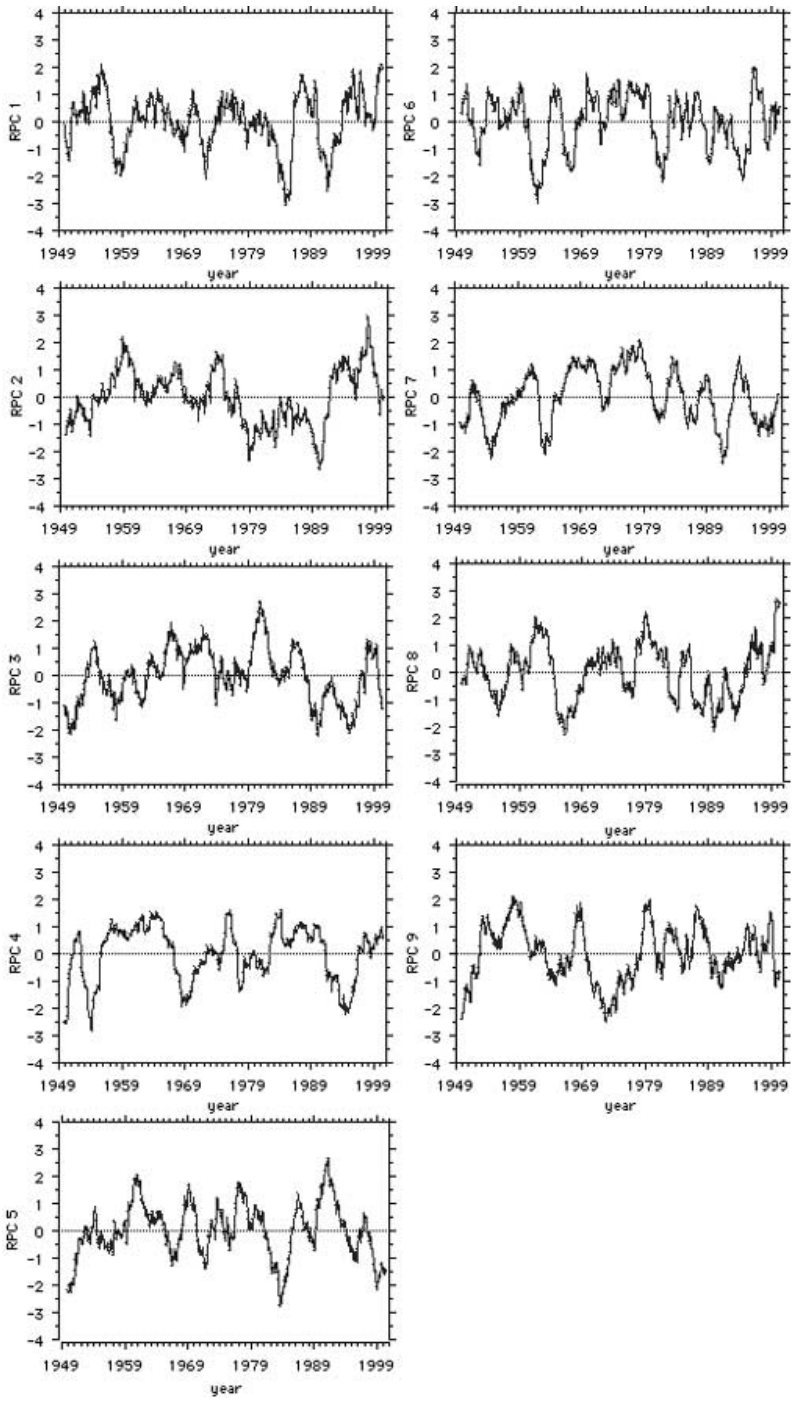

Fig. 11. – Time series of the nine VARIMAX rotated principal components (RPCs) of the SPI on a 24-month time scale. Scores are standardised. The temporal trend at each grid point has been removed.

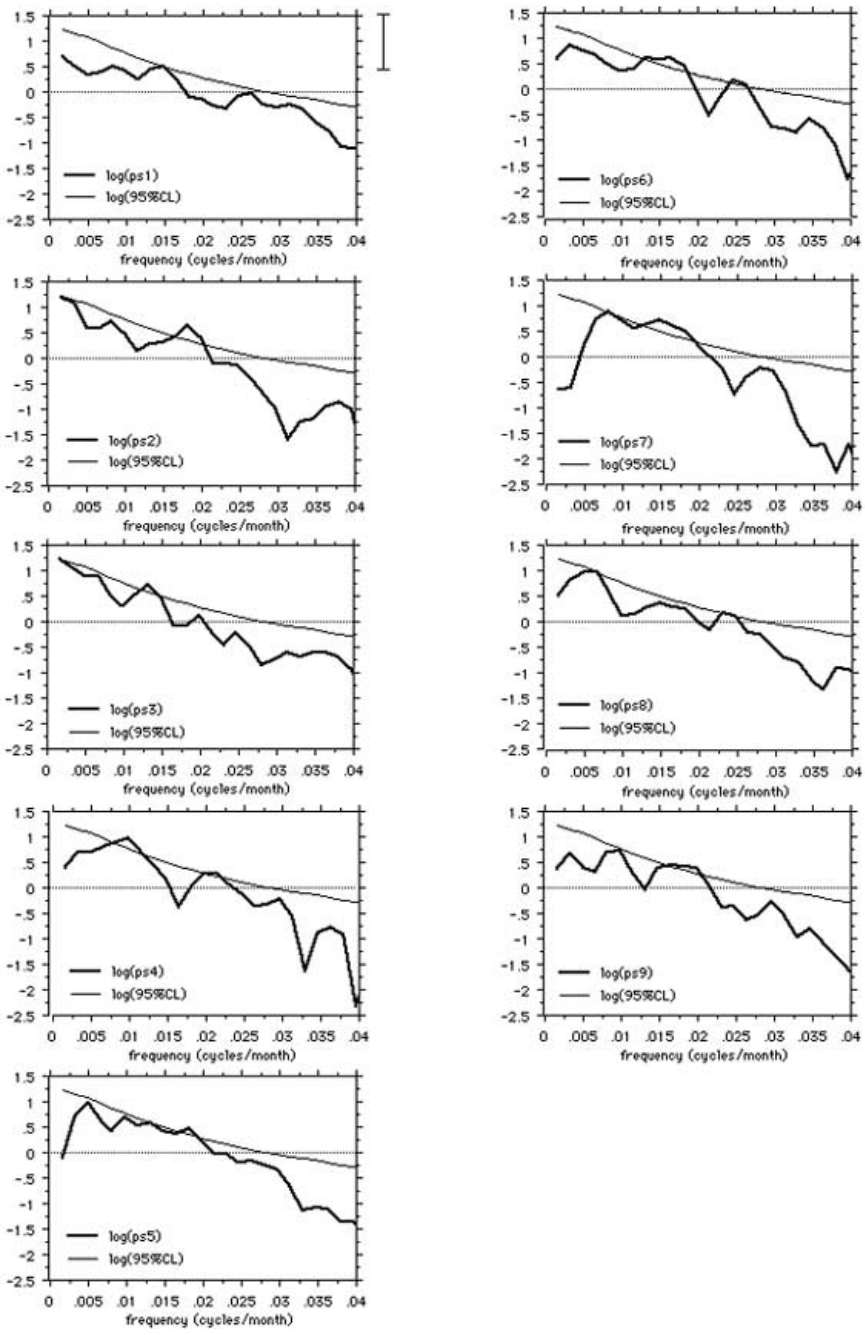

Fig. 12. – Normalised power spectra (ps) on a logarithmic scale of the nine unrotated PC scores computed by using the Tukey-Hamming spectral window at $M = 302$ lags (thick lines) as a function of frequency in cycles/month. The 95% confidence level based on the "red noise" hypothesis with 5 degrees of freedom is shown as a thin line. The vertical line on the log scale is the 95% confidence interval of the estimated scores spectra.

spectral window at $M = 302$ lags.

The results are shown in fig. 12 for each of the nine factors scores. Thick lines denote power spectra on a logarithmic scale of the nine unrotated PCs scores, while thin lines are the 95% confidence levels based on the null hypothesis that the data are generated by a "red noise" with 5 degrees of freedom ([22], p. 252; [23]). The vertical line on the log scale is the 95% confidence interval of the estimated PCs spectra. An inspection of the figures shows significant spectral peaks centred on periods of 3.3, 4.2–5.6, 7 and 8.3 years. Notice that, considering the 95% confidence intervals on a single spectral line, also other peaks might be statistical significant as the 2.7, 11 and 17 years periods.

We try to interpret these periodicities referring to the Atlantic variability.

In a recent paper Tourre *et al.* [24] identify, using a multivariate frequency analysis, the dominant spatio-temporal patterns of the joint SST and sea level pressure (SLP) variability in the Atlantic Ocean. Their results show five significant frequency bands ranging from quasi-biennial to quasi-decadal. The space and time evolution of the quasi-biennial bands, centred at 2.2 and 2.7 year periods, show that the SLP anomalies form a dipole akin to the NAO (North Atlantic Oscillation). Many authors (for example [25,26]) argued that the quasi-biennial fluctuations and the different frequencies of the Atlantic variability are linked to the southwest-northeast movement of the centres of action (*i.e.* the Icelandic low and the Azores high, often referred to as NAO). The interannual bands, centred around 3.5 and 4.4 year periods, are probably due to the link between the intensity of the tropical Atlantic trades and the ENSO phenomenon. The SST and SLP patterns associated to the quasi-decadal time scale, instead, reveal a strong NAO-SST linkage and the relationship between tropical Atlantic and the SST variability to the south and north of the ITCZ [27-29]. Moreover, Grötzner *et al.* [30] identify low-frequency variability at about 17 year period in the joint SST-SLP of the Atlantic basin and attribute it to the air-sea interactions revolving the subtropical gyre and the NAO.

The periods identified by our spectral analysis are very close to some of the time-scales mentioned above. This result allows concluding, at least, that the phenomena here observed are synchronous to some described by the previous authors. However, the physical mechanisms that could produce the connections between these fluctuations in the Tropical Atlantic and the precipitation fields in a remote area, such as the Mediterranean basin, are not clear and need further investigations.

6. – Conclusions

We have described the large-scale drought variability over the Italian region by applying the Standardized Precipitation Index on multiple time scales to the NCEP/NCAR reanalysis precipitation fields. Drought conditions in Italy for the month of August 2000 are shown as an example of the index application. The SPI computation confirms that the most important characteristics of the index are its flexibility to monitor different time scales and its standardisation. These characteristics make the SPI a useful tool to monitor short- or long-term drought's condition, and simplify the understanding of the covariance precipitation field structure.

A statistical analysis of the regions interested by drought conditions during the last fifty years reveals an increase of the percentage of dry areas in the recent three decades. Moreover, the temporal analysis of the SPI variations on a 24-month time scale by using the PCA method shows a trend toward more warm events, especially in Apulia, Calabria and Sardinia, since the late 1970s. This result is qualitatively consistent with the negative trend found by Brunetti *et al.* [31] who analysed precipitation records in Italy. Therefore,

it appears that the SPI not only is able to assess drought intensity on different regions, but also captures the climatic drift associated with the actual precipitation.

At this stage of our analysis, the physical causes of this trend remain not clear. Nevertheless, two different interpretations may be offered: either in the last thirty years all regions considered are affected by a linear decrease in precipitation, or the trend is only the descending part of a periodic behaviour, which we does not sample because of the shortness of the time series considered. We believe that a method able to distinguish between these two hypotheses is a priority in the climate research, since, being the first hypothesis correct, it is easy to foresee that the region considered will be in a dry climate in less than one hundred years.

Future efforts must be planned to study if the trend found is related to some multi-decadal variability of the climatic system and to understand if the correlation found between SOI and the leading factor score is physically motivated and statistically significant.

In order to study the natural variability of drought, we have removed the trend that characterises the SPI time series at each grid point and we have repeated the principal component analysis. Results suggest different spatial structures and temporal variability of the SPI.

By orthogonal rotation of the principal components of the SPI data, it is possible to define objectively nine regions of coherent drought variability: central-northern regions of Italy, northern Africa, western Alps, Corsica and western Tyrrhenian sea, Adriatic sea and Balkan region, Sicily and Calabria, Sardinia, northern Balkan, and finally central-eastern Alps.

A preliminary analysis of the variance spectra of the unrotated PC factor scores uncovers several periods of variability ranging from quasi-biennial to multi-decadal time scale (although for the latter the statistical confidence at 95% level is only marginal). The time scales are very close to some dominant frequencies of the Tropical Atlantic ocean variability found by Tourre *et al.* (l.c.), but the relationship between Atlantic SST and precipitation field in the Mediterranean region are not yet understood. Moreover, the spectral analysis provides no evidence for an association between moisture variability in the Italian region and the solar-related variability over the time period considered.

Further study will be directed to repeat the analysis by using global station data set of monthly precipitation and to investigate the physical origin of the trend revealed.

* * *

We thank the Department of Italian National Technical Services (DSTN) and the European Community for financial support. The authors are grateful to Prof. M. Benedini, Ing. G. Monacelli, Profs. G. Rossi, A. Speranza and P. Versace for their suggestions. Data provided by the NOAA-CIRES Climate Diagnostics Center, Boulder, Colorado, from their website at the URL http://www.cdc.noaa.gov.

REFERENCES

[1] Bordi I., Frigio S., Parenti P., Speranza A. and Sutera A., *Annali di Geofisica*, **44** (2001) 965; 979.

[2] Palmer W., *Meteorological Drought*, Tech. Rep. 45, U.S. Weather Bureau, Washington, D.C. (1965), p. 58.

[3] McKee T. B., Doesken N. J. and Kleist J., *The relationship of drought frequency and duration to time scales*, in *Preprints of 8th Conference on Applied Climatology, 17-22 January, Anaheim, CA*, 1993, pp. 179-184.
[4] Guttman N. B., *J. Am. Water Res. Assn.*, **35** (1999) 311.
[5] Kalnay E., Kanamitsu M., Kistler R., Collins W., Deaven D., Gandin L., Iredell M., Saha S., White G., Woollen J., Zhu Y., Chelliah M., Ebisuzaki W., Higgins W., Janowiak J., Mo K. C., Ropelewski C., Wang J., Leetmaa A., Reynolds R., Jenne R. and Joseph D., *Bull. Am. Meteorol. Soc.*, **77** (1996) 437.
[6] Trenberth K. E. and Guillemot C. J., *Clim. Dyn.*, **14** (1998) 213.
[7] Dai A., Fung I. Y. and Del Genio A. D., *J. Climate*, **10** (1997) 2943.
[8] Abramowitz, M. and Stegun I. A., *Handbook of Mathematical Functions* (Dover) 1965, 1046 pp.
[9] Rencher A. C., *Multivariate Statistical Inference and Applications* (John Wiley & Sons, INC.) 1998.
[10] Lorenz E. N., *Empirical Orthogonal Functions and Statistical Weather Prediction*, MIT, Dept. of Meteorology, Science Report 1 (1956).
[11] Molteni F., Sutera A. and Tronci N., *J. Atmos. Sci.*, **45** (1988) 3063.
[12] Bretherton C. S., Smith C. and Wallace J. M., *J. Climate*, **5** (1992) 541.
[13] North G. R., Bell T. L., Cahalan R. F. and Moeng F. J., *Mon. Weather Rev.*, **110** (1982) 699.
[14] IMSL 1987: STAT/LIBRARY, Fortran subroutines for statistical analysis, 1232 pp.
[15] Bordi I. and Sutera A., *Water Res. Man.*, **15** (2001) 247.
[16] Walker G. T., *Mem. Indian Meteorol. Dept.*, **24** (1924) 275.
[17] Piervitali E. and Colacino M., *Clim. Change*, **49** (2001) 225.
[18] Stockton C. W., Mitchell J. M. and Meko D. M., *A reappraisal of the 22-year drought cycle*, in McCornac B. (Editor), *Weather and Climate Responses to Solar Variations*, (Colorado University Press, Boulder, CO) 1983, pp. 507-515.
[19] Cook E. R., Meko D. M. and Stockton C. W., *J. Climate*, **10** (1997) 1343.
[20] Camuffo D., *Earth Moon and Planets*, **85** (2001) 99.
[21] Moura A. D. and Shukla J., *J. Atmos. Sci.*, **38** (1981) 2653.
[22] Jenkins G. M and Watts D. G., *Spectral Analysis and its Applications* (Holden-Day, Inc., 500 Sansome Street, San Francisco, California) 1968.
[23] Gilman D. L., Fuglister F. J. and Mitchell J. M. Jr., *J. Atmos. Sci.*, **20** (1963) 182.
[24] Tourre Y. M., Rajagopalan B. and Kushnir Y., *J. Climate*, **12** (1999) 2285.
[25] Angell J. K. and Korshover, *Mon. Weather Rev.*, **102** (1974) 669.
[26] Van Loon H. and Rogers J. C., *Mon. Weather Rev.*, **106** (1978) 296.
[27] Houghton R. W. and Tourre Y. M., *J. Climate*, **5** (1992) 765.
[28] Servain J., *J. Geophys. Res.*, **96** (1991) 15, 137, 146.
[29] Mehta V. M. and Delworth T., *J. Climate*, **8** (1995) 172.
[30] Grötzner A., Latif M. and Barnett T. P., *J. Climate*, **11** (1998) 831.
[31] Brunetti M., Colacino M., Maugeri M. and Nanni T., *Int. J. Clim.*, **21** (2001) 299.